Journal of Applied Polymer Science

Effect of double percolation on the electrical properties and electromagnetic interference shielding effectiveness of carbon-black-loaded polystyrene/ethylene vinyl acetate copolymer blends

Bluma G. Soares,[1] François Touchaleaume,[1] Loan F. Calheiros,[2] Guilherme M. O. Barra[3]

[1]Centro de Tecnologia, Programa de Engenharia Metalúrgica e Materiais, Universidade Federal do Rio de Janeiro, 21941-972 Rio de Janeiro, Brazil

[2]Instituto de Macromoléculas, Universidade Federal do Rio de Janeiro, 21941-598 Rio de Janeiro, Brazil

[3]Departamento de Engenharia Mecânica, Universidade Federal de Santa Catarina, Florianópolis Santa Catarina, Brazil

Correspondence to: B. G. Soares (E-mail: bluma@metalmat.ufrj.br)

ABSTRACT: In this study, the concept of double percolation and selective location of a conducting additive was used to develop conducting polymer composites composed of polystyrene (PS) and ethylene vinyl acetate copolymer (EVA) filled with carbon black (CB). Scanning and transmission electron microscopy suggested that the CB was preferentially located in the EVA phase. By combining a cocontinuous morphology and selective location of CB in the EVA phase, we achieved the highest conductivity values and better electromagnetic interference shielding effectiveness in the X-band frequency range for the 70:30 w/w PS/EVA blend. Electromagnetic attenuation occurred by both reflection and absorption mechanisms, although the first was predominant for composites with a higher amount of CB. The percolation thresholds of the PS, EVA, and 70:30 w/w PS/EVA blend loaded with CB were estimated from the dependence of the alternating-current and direct-current conductivities. The rheological properties were also used to relate the electrical behavior to the microstructure of the composites. © 2015 Wiley Periodicals, Inc. J. Appl. Polym. Sci. **2016**, *133*, 43013.

KEYWORDS: blends; composites; conducting polymer; dielectric properties

Received 2 July 2015; accepted 2 October 2015

DOI: 10.1002/app.43013

INTRODUCTION

Conducting polymer composites are composed of a conductive filler dispersed into an insulating matrix; they have attracted great interest because of their versatility of applications in different fields, such as antistatic devices for the dissipation of electrostatic charges, electromagnetic interference (EMI) shielding materials, capacitor, and sensors. Such properties depend on the electrical conductivity degree, which can be easily tuned by the appropriate choice of the polymeric matrix, conductive filler nature and proportion, and blending conditions. These systems usually present a defined insulating–conducting transition at a critical amount of conductive filler, known as the *percolation threshold point*.[1] Among several conducting fillers, carbon black (CB) is still considered one of the most popular because of its low cost and chemical stability. Depending on the polymer matrix, the amount of CB necessary to achieve a desirable electrical conductivity is high; this results in an increase in the melt viscosity and a decrease in the mechanical performance of the final product. The use of heterogeneous polymer blends in cocontinuous morphology has been well described as an efficient approach for attaining good electrical conductivity with the lowest amount of conducting filler.[2] Such a strategy is based on an early statement by Sumita *et al.*[3] that CB may be selectively located in one phase or at the interface of a heterogeneous polymer blend. The factors driving the preferential localization of the CB are thermodynamics, kinetics, and polymer melt viscosity. The thermodynamic approach predicts the preferential localization of the filler, which depends on the free energy of the various interfaces. This prediction is quantitatively formalized by the calculation of the wetting coefficient.[4] The kinetic contribution is directly linked to the processing conditions. The final morphology of the material may differ from the thermodynamically predicted one because the viscosities encountered in such systems require very high residence times for the thermodynamic equilibrium to be set up and the filler to migrate in the preferred location.[5] In addition to the key thermodynamic and kinetic contributions, it has been reported that the less viscous phase may be preferred as a location for such fillers.[6,7]

The confinement of CB particles in one of the continuous phases or, better, at the interface of a heterogeneous and cocontinuous polymer blend should produce conducting pathway formation at a lower CB loading. This phenomenon is known as

double percolation and is characterized by the percolation of the polymer phases and the conducting particles.[8–10]

The demand of high-quality materials that can shield the external EMI has continuously increased because of the development of sophisticated electronic devices that produce electromagnetic radiation that may interfere with the performance of other equipment. The EMI shielding effectiveness (SE) is strongly influenced by the electrical conductivity of the composite and by the dielectric properties, composite shape, conducting particle dispersion, and so on. Therefore, it is expected that a conducting-additive-loaded heterogeneous polymer blend should display a higher EMI SE as a consequence of its higher conductivity, provided by the double-percolation phenomenon, and associated with the selective location of the conducting filler at one continuous phase or at the interface of such a blend. Although double percolation has been extensively reported, very few articles have related the EMI SE with the double-percolation phenomenon and cocontinuity in heterogeneous polymer blends. Some studies have dealt with the evaluation of EMI SE in heterogeneous blends loaded with conducting additives without examination of the cocontinuous composition.[11–14] Rohini and Bose[15] described the outstanding EMI SE in a polystyrene (PS)/poly(methyl methacrylate) (50:50 w/w) blend loaded with multiwalled carbon nanotube (MWCNTs) and suggested the selective location of the MWCNTs in the PMMA phase of a cocontinous blend morphology. The polycarbonate (PC)/acrylonitrile-butadiene-styrene copolymer (ABS) blends loaded with MWCNTs were also studied for EMI SE.[16] From microscopic studies, the authors suggested the selective location of MWCNTs in the ABS phase and a good EMI SE. However, only the PC/ABS (80:20 w/w) composition was studied. Recently, an EMI SE between −5 and −15 dB was reported with MWCNTs with different surface modifications in PC/SAN (50:50 w/w) blend.[17] This composition was situated in the cocontinuous range morphology. In an interesting report published by Al-Saleh and Sundararaj,[18] a polypropylene/PS blend loaded with CB was studied under different compositions. They observed a preferential location of CB inside the PS phase and a cocontinuous morphology of the PP/PS blends corresponding to compositions of 50:50 and 75:25 w/w. However, a higher electrical conductivity and EMI SE were observed when pure PP was used as the matrix; this was in contrast to the double-percolation theory.

From the results published in the literature, studies related to conducting polymers for EMI shielding applications still deserve some attention and additional study. Therefore, the aim of this study was to highlight the importance of the double-percolation threshold in PS/ethylene vinyl acetate copolymer (EVA) blends loaded with CB to achieve better conductivity and EMI SE. The choice of the PS/EVA blends was based on their wide range of compositions with cocontinuous structures.[19] Additionally, EVA is known to improve the processability and toughness of polymer blends because of its elastomeric characteristics, which can be tuned by changes in the vinyl acetate content in the copolymer. EMI SE of these CB-loaded heterogeneous blends was related to the cocontinuous morphology. The percolation threshold of the blends in the cocontinuous morphology was compared with those corresponding to the CB-loaded PS or EVA blends. Also, the electrical percolation threshold was compared with the rheological behavior and EMI SE for ternary and binary blends.

EXPERIMENTAL

Materials

PS (melt flow index = 6.13 g/10 min at 200°C/2.16 kg) was purchased from Companhia de Estireno do Brasil. EVA (melt flow index = 2.5 g/10 min at 190°C/2.16 kg, vinyl acetate content = 18 wt %) was purchased by Braskem (Brasil). CB (Printex XE2, DBP = 370 mL/100 g, specific surface area = 1000 m^2/g, density = 2.04–2.11 g/cm^3) was supplied by Degussa.

Blend Preparation

PS, EVA, and CB were vacuum-dried overnight before they were introduced into the chamber of a Brabender plastograph equipped with a W50 EHT internal mixer and roller rotors working at 170°C and 60 rpm. The mixing was performed for 10 min. After that, the material was milled and compression-molded in a hydraulic press at 200°C and 6 MPa for 3 min; this was followed by cooling at the same pressure.

Characterization

The rheological study of the blends was carried out at 200°C with a Physica MRC302 rheometer from Anton Paar disposed with parallel plates 25 mm in diameter and with a gap of 1000 μm. The measurements were performed in oscillatory mode at a frequency range from 10^{-1} to 10^2 Hz and amplitude of 1%.

The direct-current (dc) electrical conductivity was measured in an Agilent high-resistance meter (model 4339B) with a two-probe standard method with electrodes 25 mm in diameter and samples 1 mm in thickness. For composites with high conductivities, the measurements were performed with the four-probe standard method with a Keithley 6220 current source to apply the current and a Keithley 6517A electrometer to measure the potential difference method. All of the measurements were performed at room temperature five times, and the electrical conductivity values were averaged.

The alternating-current (ac) conductivity was measured with a Solartron SI 1260 gain phase analyzer interfaced to a Solartron 1296 dielectric interface. The measurements were performed at room temperature in a frequency range of 0.1 Hz to 10 MHz with a 5-V oscillating voltage with electrodes 25 mm in diameter. Samples 1 mm in thickness were used.

EMI SE was evaluated in the X-band microwave range (8.2–12.4 GHz) with a network analyzer type N5230L PNA-L with a rectangular waveguide. The samples 1 mm in thickness were compression-molded.

Scanning electron microscopy (SEM) was performed in a JEOL 2000 FX microscope with an accelerator power of 20 kV. The samples were cryofractured, and the surfaces were treated previously with methyl ethyl ketone (MEK) to selectively extract the PS phase. Then, the surface was coated with a thin layer of gold and analyzed.

Transmission electron microscopy (TEM) was performed on an FEI-Titan G2 80-200 microscope at 80 kV. The samples were

Table I. Surface Energies and Polarities of the Polymers and CB

Sample	γ (mJ m^{-2})	γ^d (mJ m^{-2})	γ^p (mJ m^{-2})	χ^p (%)
PE	35.7	35.7	0	0.0
PVA	36.5	25.1	11.4	31.2
EVA (14 mol % vinyl acetate)	35.8	34.2	1.6	4.5
PS	40.6	34.5	6.1	15.0
CB	108.8	108.1	0.7	0.6

γ = surface free energy; γ^d = dispersive component of the surface energy; γ^p = polar component of the surface energy; χ^p = contribution of the polar component of surface free energy.

prepared with an RMC ultracryomicrotome equipped with a diamond knife to obtain 80 nm thick ultrathin sections.

RESULTS AND DISCUSSION

Calculation of the Wetting Coefficient

The thermodynamically favored localization of the filler could quantitatively be predicted by the value of the wetting coefficient (ω_a) of the ternary system, defined as follows[3]:

$$\omega_a = \frac{\gamma_{CB/PS} - \gamma_{CB/EVA}}{\gamma_{PS/EVA}} \quad (1)$$

where $\gamma_{CB/PS}$, $\gamma_{CB/EVA}$, and $\gamma_{PS/EVA}$ represent the interfacial tensions between CB and the PS matrix, between CB and the EVA matrix, and between PS and EVA, respectively. When ω_a is greater than 1, CB is preferentially distributed among the EVA phase. When ω_a is less than -1, the PS phase is preferred, and in the intermediary case, the CB is located at the interphase.

The interfacial energies ($\gamma_{A/B}$) were calculated from the surface energies with two widely used methods: the geometric mean equation[20]

$$\gamma_{A/B} = \gamma_A + \gamma_B - 4\left(\frac{\gamma_A^d \gamma_B^d}{\gamma_A^d + \gamma_B^d} + \frac{\gamma_A^p \gamma_B^p}{\gamma_A^p + \gamma_B^p}\right) \quad (2)$$

and the harmonic mean equation:

$$\gamma_{A/B} = \gamma_A + \gamma_B - 2\left(\sqrt{\gamma_A^d \gamma_B^d} + \sqrt{\gamma_A^p \gamma_B^p}\right) \quad (3)$$

where γ_A and γ_B are the surface energies of components A and B, respectively; $\gamma_A{}^d$ and $\gamma_B{}^d$ are the dispersive components of γ_A and γ_B, respectively; and $\gamma_A{}^p$ and $\gamma_B{}^p$ are the polar components of γ_A and γ_B, respectively.

The surface free energies of PS and CB are available in the literature,[7,21] and for the surface free energy of EVA (γ_{EVA}; containing 19 wt % vinyl acetate, i.e., 14 mol %), an arithmetic mean value was calculated from the polyethylene (PE) and poly(vinyl acetate) (PVA) values[7]:

$$\gamma_{EVA} = x_{PE} \times \gamma_{PE} + x_{PVA} \times \gamma_{PVA} \quad (4)$$

where x_{PE} and x_{PVA} are the molar fractions of PE and PVA, respectively, and γ_{PE} and γ_{PVA} are the surface tensions of PE and PVA, respectively. The surface energies of the materials and interfacial energies calculated with the two previously detailed equations are reported in Tables I and II, respectively.

Table II. Interfacial Energies Calculated from the Geometric Mean and Harmonic Mean Equations

	Interfacial energy (mJ m^{-2})	
	Geometric mean	Harmonic mean
PS/EVA	1.4	2.6
CB/PS	23.1	42.3
CB/EVA	20.9	38.7

Calculations of the wetting coefficient for the PS/EVA/CB system provided values of 1.56 when the geometric mean equation was used and 1.35 when the harmonic mean equation was used. Those values, higher than 1, indicated that in the thermodynamic equilibrium, CB particles were preferentially located in the EVA phase.

Electrical Conductivity and Morphology

Figure 1 displays the dc electrical conductivity of PS/EVA blends containing 5 wt % CB as a function of the blend composition. The conductivity level of all of the blends was quite similar in a wide range of compositions (from 20 to 80 wt % EVA), probably because of the relatively high amount of CB used in this study. However, the 70:30 w/w PS/EVA blend displayed a slight increase in the conductivity value related to the other blends (0.014 S/cm). According to previous work,[19] PS/EVA blends present a cocontinuous morphology in a wide range of compositions. Therefore, the maximum of conductivity found in the 70:30 w/w PS/EVA was attributed to the double percolation. As both phases were continuous and the CB particles were selectively located in the minor phase (30 wt % EVA), the particles were able to touch each other; this made the formation of a conducting network easier. As discussed later, this specific composition also provided the highest EMI SE and confirmed the importance of conductivity to attain a better EMI SE.

Figure 2 presents the SEM micrographs of the 70:30 w/w PS/EVA blends, which were previously extracted with MEK to eliminate the PS phase. In both the CB-loaded and unloaded blends, the cocontinuous structure was evident. However, the presence of CB

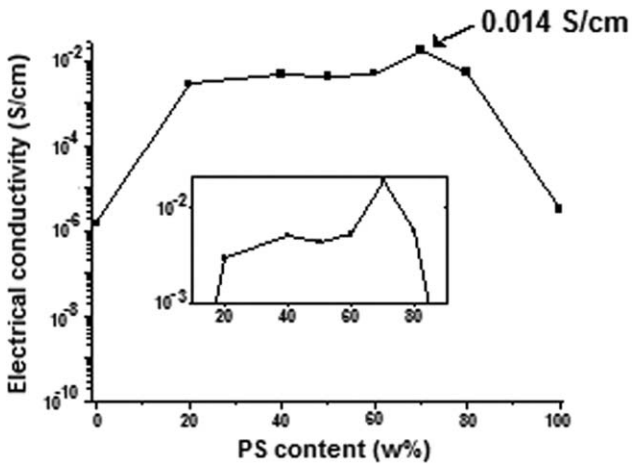

Figure 1. dc conductivity values of the PS/EVA blends loaded with 5 wt % CB as a function of the blend composition.

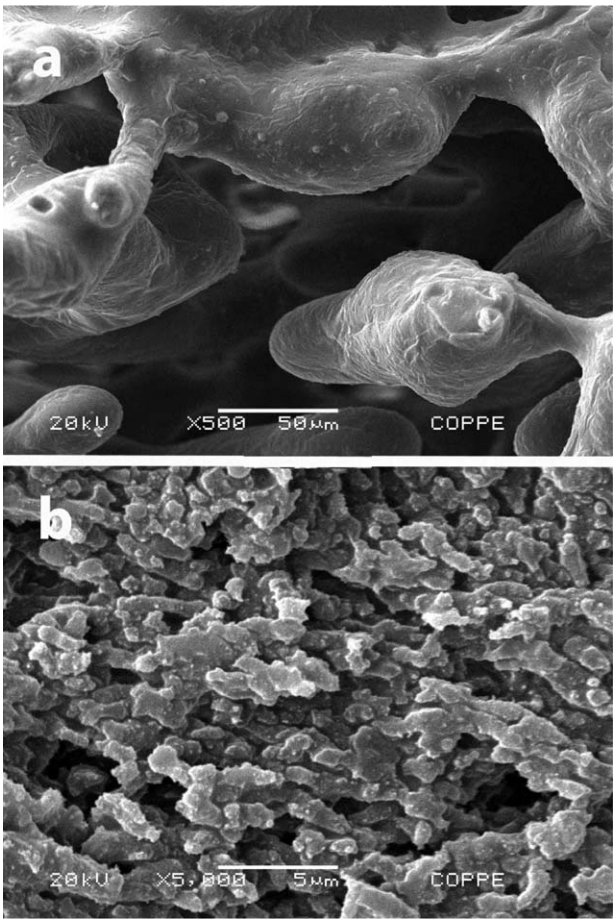

Figure 2. SEM micrographs of the PS/EVA (70:30 w/w) blends whose PS phase was selectively extracted with MEK: (a) unloaded (500×) and (b) loaded with 5 wt % CB (5000×).

significantly affected the morphology. The micrograph of the unloaded blend [Figure 2(a)] taken at a lower magnification (500×) displayed the nonextracted EVA phase as a continuous morphology with an average diameter higher than 50 µm. On the other hand, the micrograph of the CB-loaded blend taken at a higher magnification (5000×) presented a thin and elongated continuous EVA phase with an average diameter in the range 0.5–2.5 µm. These results suggest that CB acted as an interfacial agent, decreasing the chance of coalescence of the PS and EVA phase. In Figure 2(b), it is also possible to observe several white spots on the EVA phase and the interface; this corresponded to the CB particles and indicated the selective location of CB in the EVA phase, as previously predicted by calculations of the wetting coefficient.

To confirm the selective location of CB within the EVA phase, TEM of the sample containing 5.0 wt % CB was also recorded, and the micrograph is shown in Figure 3. The presence of the CB nanoparticles as aggregates confined in the EVA continuous phase was clearly observed. These results confirmed the interfacial action of CB, which diminished the chance of coalescence of the PS and EVA phases and the selective location of CB within the EVA phase.

In addition to the thermodynamic considerations based on the wetting coefficient calculations, the rheological approach had to

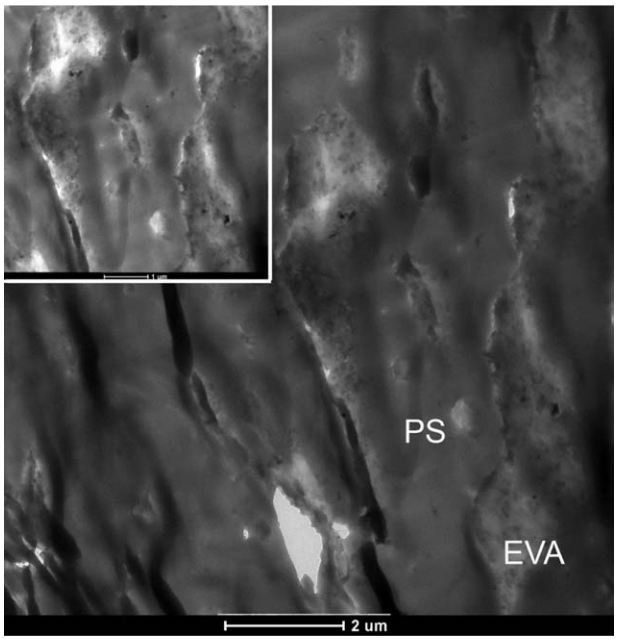

Figure 3. TEM micrograph of PS/EVA (70:30 w/w) composites loaded with 5 wt % CB.

be taken into account. Usually, CB particles tend to be located in the lower melt-viscosity phase of a heterophase blend. According to the rheological data, which is discussed later, the melt viscosity of EVA was lower than that of PS at the processing temperature; this explained the preferential location of the filler in the EVA phase. The confinement of CB in the thin EVA phase should have been responsible for the formation of the conducting network and the increase in the conductivity for this sample.

Investigations related to the percolation threshold of the PS/CB, EVA/CB, and PS/EVA/CB composites were performed by the measurement of both the dc and ac electrical conductivities. For these studies, the 70:30 w/w PS/EVA composite was chosen because this composition resulted in a better electrical conductivity, as shown in Figure 1. Figure 4 illustrates the dependence of the dc conductivity as a function of the amount of CB. All of the systems exhibited an improvement of the electrical conductivity with increasing loading of CB, as expected. The EVA/CB system (curve b) presented a little higher conductivity at 5% CB than the PS/CB system. However, for all of the CB contents, the PS/EVA (70:30 w/w) composite displayed a much higher conductivity than the neat PS and EVA composites; this confirmed the double-percolation effect (cocontinuity and conducting pathway), as observed in the SEM and TEM micrographs.

The ac electrical conductivity was also investigated to confirm the electrical percolation threshold of the CB-loaded PS, EVA, and PS/EVA (70:30 w/w) composites, whose behavior as a function of the frequency is illustrated in Figure 5. Also, Table III exhibits the dc electrical conductivity and ac conductivity at a frequency of 10 Hz. Pure polymers and the blend without CB presented an almost linear dependence of the conductivity with frequency; this confirmed the insulating nature of these matrices. A similar behavior was also observed for the PS or EVA

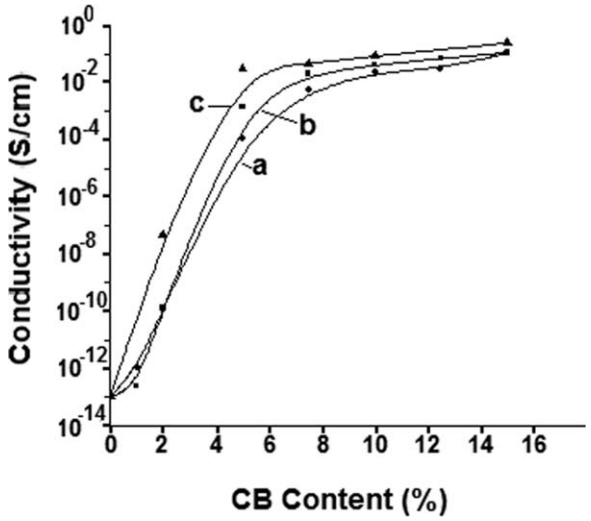

Figure 4. Effect of the CB content on the dc electrical conductivity of the CB-loaded (a) PS, (b) EVA, and (c) PS/EVA (70:30 w/w) composites.

composites containing 2% CB, although the EVA/CB composite exhibited a higher ac conductivity value; this confirmed the results previously observed for the dc electrical conductivity. For such systems, the ac conductivity was mainly governed by the interfacial polarization process; this originated from the polar differences between the filler and matrix. After this composition, there was a sharp increase in the conductivity at lower frequencies; these values were also independent of the frequency. That is, the conduction began to show an ohmic mechanism.[22] This drastic change in the conductivity values at low frequencies corresponded to the percolation threshold phenomenon. From these results, it was possible to assume that the insulating–conducting transition point was between 2 and 5% CB for the PS- or EVA-based composites. However, for the PS/EVA composites, the conductivity values did not depend on the frequency for all of the CB proportions studied; this indicated that the percolation threshold point was lower than 2% and highlighted the importance of the double percolation for attaining better conductivity values.

Rheology

Rheology measurements constitute an important method for assessing the microstructure of composites loaded with microparticles and nanoparticles. Figure 6 compares the variation in the complex viscosity with the angular frequency for PS/EVA blends with pure components. With regard to the unloaded blend components [Figure 6(a)], the EVA matrix presented a lower viscosity (450 Pa s at 10 rad/s) than PS (700 Pa s at 10 rad/s); this confirmed the predicted preferential location of CB inside the EVA phase in the filled blends.[23]

The viscosities of the filled PS/EVA composites presented higher values than those found for the filled binary composites (PS/CB and EVA/CB). As an example, the viscosity values of the PS/EVA, PS, and EVA composites loaded with 15% CB at 10 rad/s were 22.3, 14.7, and 11.3 KPa s, respectively. This behavior was observed for all of the filled blends with different CB contents; this suggested that the presence of a conductive network provided by the CB particles acted as a reinforcing agent for the PS/EVA blends.

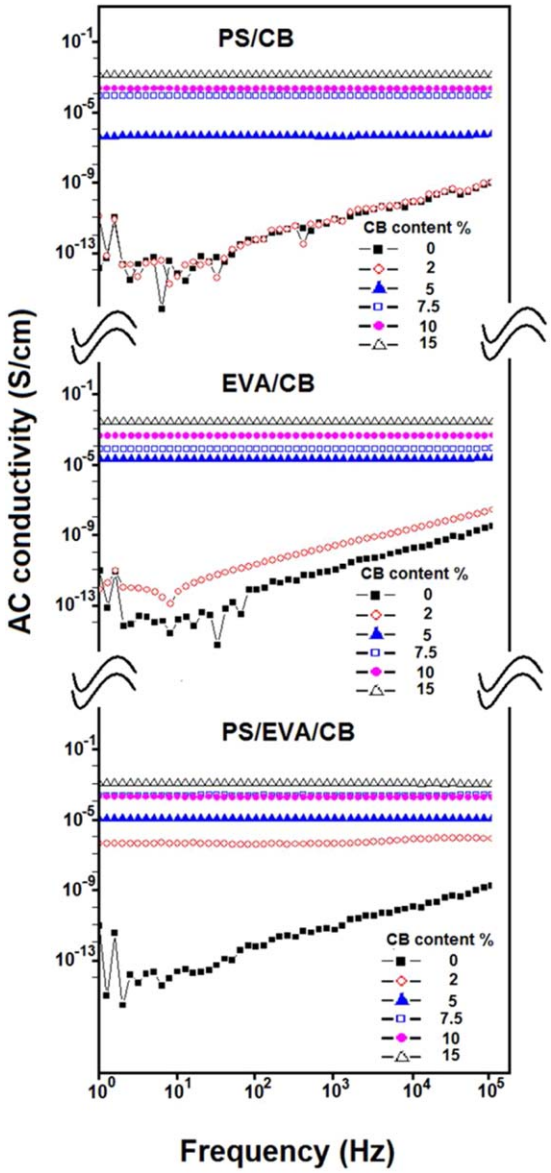

Figure 5. Effect of the CB content on the ac conductivity of the CB-loaded PS, EVA, and PS/EVA (70:30 w/w) blends. [Color figure can be viewed in the online issue, which is available at wileyonlinelibrary.com.]

The behavior of the storage modulus (G') with the angular frequency provided important information with regard to the distribution of particles in a polymer system.[24,25] Figure 7 illustrates the variation of G' with the angular frequency for the PS/CB, PS/CB, and PS/EVA/CB blends. All of the composites presented gradual increases in G' as the amount of CB increased, and this behavior was more important at low frequencies and indicated the development of the CB network with increasing filler content.[26,27] It was possible to observe a significant increase in G' between the unloaded systems and those containing only 2% CB; this suggested that the filler network structure started to form in this CB content range. That is, the rheological percolation was envisaged in this composition range. This difference was higher for the PS/EVA blends and indicated the formation of the filler conducting network

Table III. Electrical Conductivity of the PS-, EVA- and PS/EVA (70:30 w/w)-Based Composites as a Function of the CB Content

Composite component				
PS (wt %)	EVA (wt %)	CB (wt %)	dc conductivity (S/cm)	ac conductivity at 10 Hz (S/cm)
100	0	0	1.0×10^{-13}	1.3×10^{-15}
99	0	1	1.0×10^{-12}	—
98	0	2	1.1×10^{-10}	1.6×10^{-14}
95	0	5	1.1×10^{-4}	4.1×10^{-7}
92.5	0	7.5	5.4×10^{-3}	7.7×10^{-5}
90	0	10	2.3×10^{-2}	2.1×10^{-4}
87.5	0	12.5	3.1×10^{-2}	—
85	0	15	1.1×10^{-1}	1.0×10^{-3}
0	100	0	1.0×10^{-13}	1.3×10^{-14}
0	99	1	2.3×10^{-13}	—
0	98	2	1.4×10^{-10}	6.2×10^{-13}
0	95	5	1.4×10^{-3}	1.8×10^{-5}
0	92.5	7.5	2.0×10^{-2}	7.0×10^{-5}
0	90	10	4.1×10^{-2}	3.6×10^{-4}
0	87.5	12.5	7.0×10^{-2}	—
0	85	15	1.1×10^{-1}	2.5×10^{-3}
70	30	0	1.3×10^{-13}	1.9×10^{-14}
68.6	29.4	2.0	4.5×10^{-8}	4.6×10^{-7}
66.5	28.5	5.0	3.3×10^{-2}	9.8×10^{-6}
64.75	27.75	7.5	4.8×10^{-2}	1.6×10^{-4}
63.0	27.0	10.0	8.5×10^{-2}	2.3×10^{-4}
59.5	25.5	15.0	2.4×10^{-1}	1.0×10^{-3}

at a lower CB content; this agreed with the electrical percolation discussed in the previous section. As the amount of CB content increased, G' also increased and became less dependent on the frequency. In all of the CB compositions that we used, G' was higher for the PS/EVA blends; this confirmed the higher network structure formed in the cocontinuous blend.[26,28]

EMI SE

The effect of the PS/EVA blend composition on the overall EMI SE at 10 GHz is illustrated in Figure 8, for composites containing 5% of CB. The EMI SE increases with the amount of PS in the blend and reaches maximum value at 70:30 w/w PS/EVA blend (8.7 dB). This composition also displays the highest electrical conductivity, as illustrated in Figure 1, and emphasized

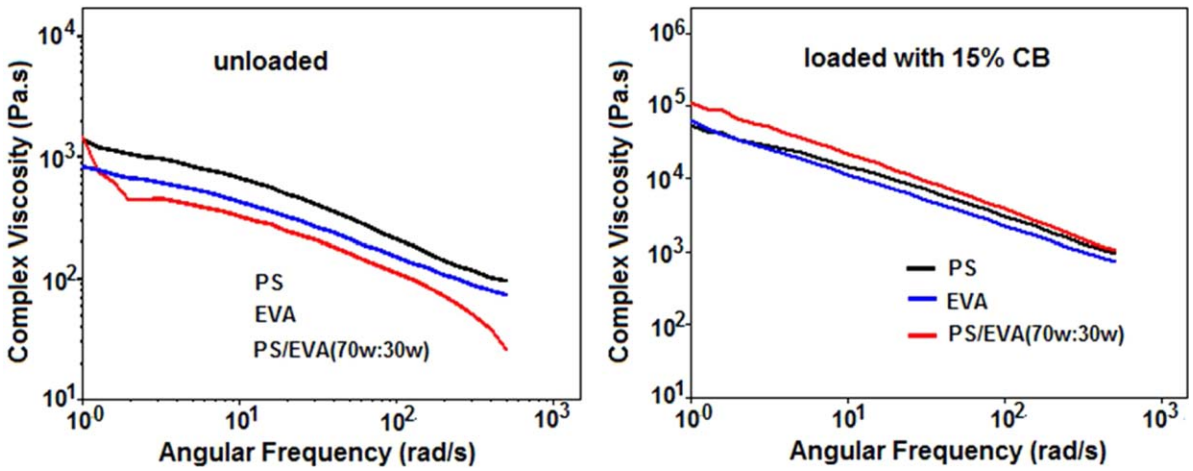

Figure 6. Dependence of the viscosity on the angular frequency for the (A) unloaded PS, EVA, and PS/EVA blend matrices and (B) 15% CB-loaded PS, EVA, and PS/EVA blend matrices. [Color figure can be viewed in the online issue, which is available at wileyonlinelibrary.com.]

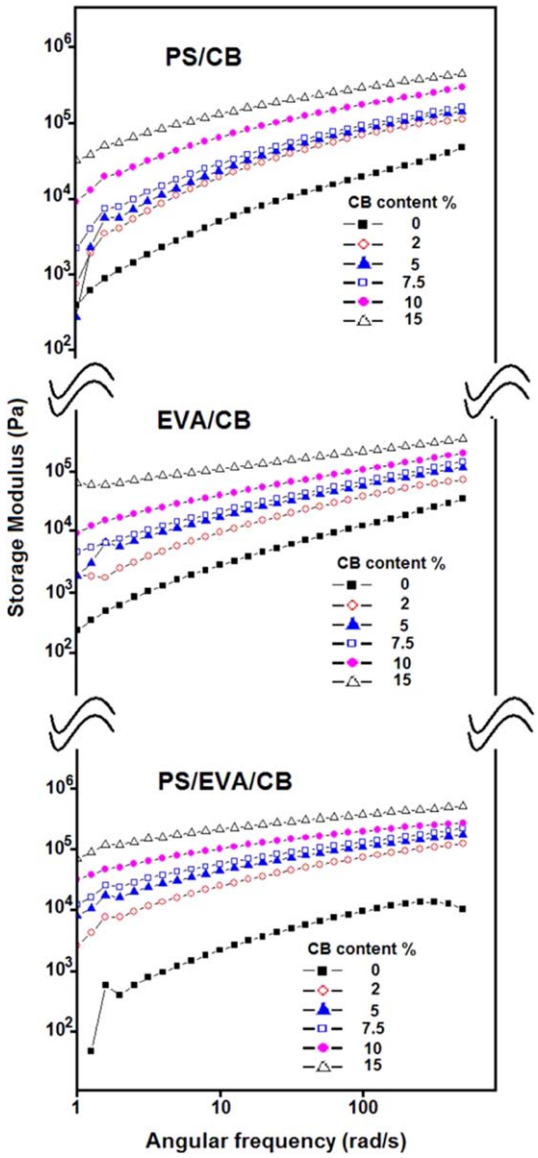

Figure 7. G′ as a function of the angular frequency for the PS, EVA, and PS/EVA (70:30 w/w) blends containing different amounts of CB. [Color figure can be viewed in the online issue, which is available at wileyonlinelibrary.com.]

the importance of double percolation for reaching better conductivity values and EMI SE.

The effect of the CB content on the overall EMI SE was evaluated for the PS, EVA, and 70:30 w/w PS/EVA composites in the X-band, as illustrated in Figure 9. As expected, the increase in the CB content increased the EMI SE because of the conducting character of CB, whose charge carriers moved freely and interacted directly with the incident electromagnetic field; this contributed to the electromagnetic wave attenuation. For systems with CB contents higher than 5%, the increase in the conductivity was marginal, whereas the EMI SE significantly increased. Beyond this composition, the continuous conducting network was already formed, and an increase in the CB content only contributed to an increase in the number of the conducting pathways. However, the networks became denser and

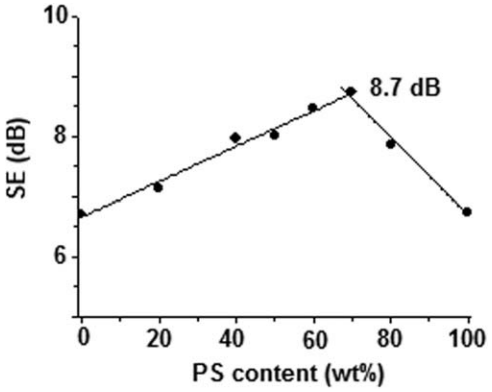

Figure 8. Variation of EMI SE with the composition of the PS/EVA blends filled with 5% CB as measured at 10 GHz.

denser; this prevented the penetration of electromagnetic radiation and, thus, improved the EMI SE.

The presence of 2 wt % CB on 70:30 w/w PS/EVA composite exerted a greater influence on the EMI SE than those related to the PS- and EVA-based composites with similar amounts of CB. At this CB content, the PS/EVA composite already displayed a conducting network, as indicated by the electrical conductivity behavior discussed in the previous section; this contributed to a

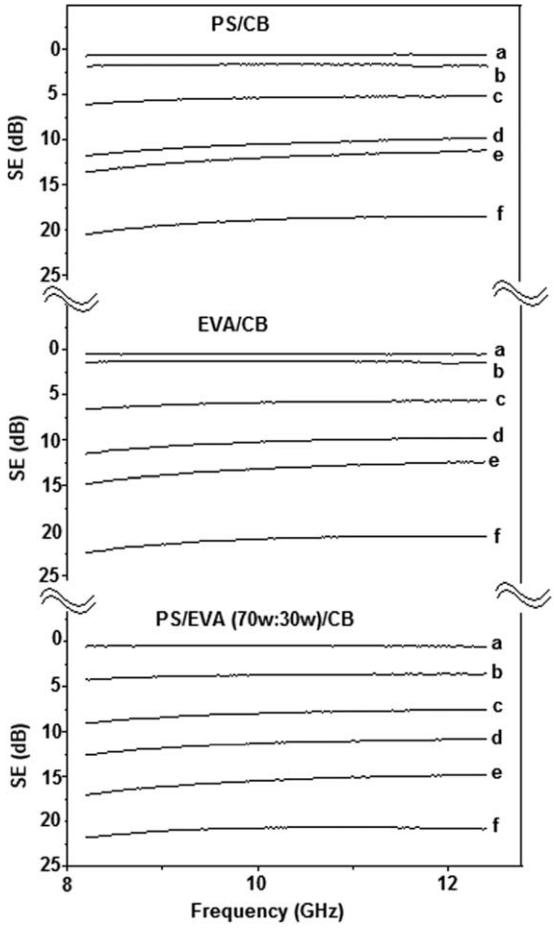

Figure 9. Overall EMI SE of the PS, EVA, and PS/EVA (70:30 w/w) blends containing different amounts of CB: (a) 0, (b) 2, (c) 5, (d) 7.5, (e) 10, and (f) 15%.

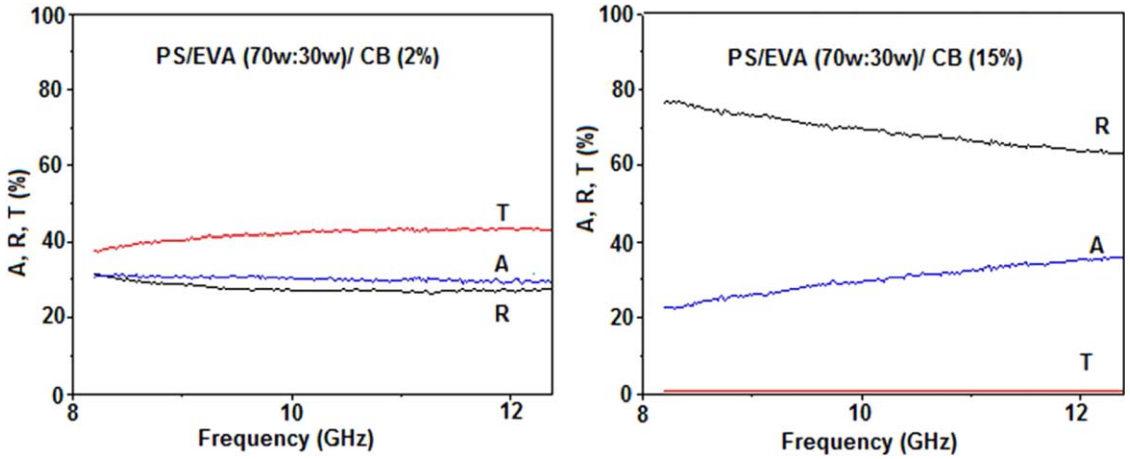

Figure 10. Percentage of *T*, *A*, and *R* in the X-band frequency range for the PS/EVA (70:30 w/w) blends with a 1-mm thickness. [Color figure can be viewed in the online issue, which is available at wileyonlinelibrary.com.]

significant improvement in the EMI SE, as compared with the binary PS/CB or EVA/CB composites. With increasing CB content, the EMI SE also increased as the conducting network became denser. For CB contents as high as 15%, the EMI SE of the 70:30 w/w PS/EVA blend was similar to that found for the EVA/CB composites and a little higher than that corresponding to the PS/CB composites; this indicated that at this CB proportion, a similar and dense conducting network was formed in both the EVA and 70:30 w/w PS/EVA blend matrices. At this composition, the EVA phase in the PS/EVA composite was saturated with the conducting filler, and the conducting network was well distributed in both the PS and EVA phases.

When electromagnetic radiation finds a material, it undergoes different effects, such as transmission power (T) through the material, reflection power (R), and absorption power (A) by the material. The overall EMI SE results from a combination of all of these processes. The scattering parameters S_{21} (S_{12}) and S_{11} (S_{22}) obtained from the network analyzer provide the T and R, respectively, according to the following equations[29,30]:

$$\mathrm{PT}=\mathrm{PI}\left|{}^{E_t}/_{E_i}\right|^2=\mathrm{PI}|S_{12}|^2 \tag{5}$$

$$\mathrm{PR}=\mathrm{PI}\left|{}^{E_R}/_{E_i}\right|^2=\mathrm{PI}|S_{11}|^2 \tag{6}$$

where E_t = transmitted electromagnetic radiation; E_i = incident electromagnetic radiation; E_R = reflected electromagnetic radiation.

A is then determined by the following equation:

$$\mathrm{PA}=\mathrm{PI}-(\mathrm{PR}+\mathrm{PT}) \tag{7}$$

where PR is the reflection power obtained from S_{11} (S_{22}), PT is the transmission power obtained from S_{21} (S_{12}), and PI is the power of incident radiation. For application purposes, it is very important to determine the percentage of each event exerted by the material in contact with an electromagnetic wave.

Figure 10 illustrates the percentage of each event for the 70:30 w/w PS/EVA blends containing 2 and 15% CB. For the sample with 2% CB, the main event was *T*, but there were great percentages of *A* and *R* of the EM radiation by the composite. At this low amount of CB, the effect was similar in the entire frequency range studied. Despite the conducting network already formed, the structure presented several spaces that could facilitate the penetration of electromagnetic radiation. Therefore, the *A* phenomenon was more important. With increasing CB content, the EMI shielding was significantly more effective, as indicated by the very low percentage of *T*. However, the main attenuation phenomenon was related to *R* because of the formation of a dense conducting network; this resulted in an increase in the amount of charge carriers in the conducting filler. These charge carriers interacted directly with the incident wave and contributed to the *R* mechanism. Similar behavior was also reported by Al-Saleh and Sundararaj[31] for systems constituted by polypropylene and MWCNTs. According to those authors, the lower *A* was a consequence of the lower power transmitted into the

Table IV. Effect of CB on the Percentage of Absorbed, Reflected, and Transmitted Radiation of the PS/EVA (70:30 w/w) Composites at 10 and 12 GHz as a Function of the Amount of CB

			10 GHz					12 GHz				
PS (wt %)	EVA (wt %)	CB (wt %)	SE (dB)	*A* (%)	*R* (%)	*T* (%)	*R*/*A*	SE (dB)	*A* (%)	*R* (%)	*T* (%)	*R*/*A*
68.6	29.4	2.0	0.5	31	27	42	0.86	0.6	30	27	43	0.90
66.5	28.5	5.0	8.0	35	49	16	1.40	7.5	35	47	18	1.30
64.75	27.75	7.5	11.4	34	59	7	1.73	10.9	40	51	9	1.27
63.0	27.0	10.0	15.5	36	61	3	1.69	15.0	42	55	3	1.31
59.5	25.5	15.0	20.8	29	70	1	2.41	20.8	35	64	1	1.82

sample because of the better *R*. On the basis of the EMI SE theory, mobile charge carriers were responsible for the *R* effect and increased in importance for the systems with higher conductivities.[32,33] At high amounts of CB, the *R* decreased as the frequency increased, and *A* increased. This behavior may have been due to the lower wavelength of the electromagnetic radiation, which could penetrate into the material more easily. This resulted in better interaction between the radiation and the material. Liu *et al.*[34] also observed similar behavior for carbon nanotube/polyurethane composites and attributed this to the contribution of the increase in the dielectric loss of the composite. The *A*, *R*, and *T* contributions and the overall EMI SE values at frequencies of 10 and 12 GHz are summarized in Table IV. All composites presented contributions of both *A* and *R* mechanisms to the overall EMI SE; this suggested that these materials were good electromagnetic absorbers and are interesting for military applications. It was interesting to observe that the attenuation mechanism for the blend with 2% CB was mainly *A*. When the amount of CB increased, the *R* phenomenon became more important. These results were explained by the increase in the conducting filler amount; this also increased the amount of charge carriers interacting with the electromagnetic radiation. Although *R* is an important event, the *R*/*A* ratio was not so high; this suggested that these materials were good absorbers, mainly at higher frequencies, where this ratio was lower.

CONCLUSIONS

PS/EVA blends with different compositions and loaded with CB were developed to establish compositions for attaining better electrical conductivity and a higher EMI SE. Although the PS/EVA blends presented a wide range of cocontinuous compositions, the best performance in terms of the electrical conductivity and EMI SE was observed for the 70:30 w/w PS/EVA blend; this was attributed to the double percolation, that is, the cocontinuous structure of the blend associated with the selective location of CB at the EVA phase; this was the minor phase in this cocontinuous blend. The rheological properties were also measured in terms of the viscosity and G', and the results obtained from the percolation threshold obtained from the ac electrical conductivity and rheological measurements were in agreement.

The EMI SE values of the PS, EVA, and 70:30 w/w PS/EVA blends containing 15% CB stayed around 20 dB with samples 1 mm in thickness and should be considered very good for most applications. The electromagnetic wave attenuation occurred by *A* and *R*, although *R* was somewhat predominant, mainly for higher amounts of CB; this was is attributed to the denser conducting structure, thus increasing the amount of charge able to interact with the electromagnetic radiation. Finally, in this article, we highlight the importance of the morphology and conductivity in attaining a good EMI SE.

ACKNOWLEDGMENTS

This work was sponsored by the following agencies in Brazil: Conselho Nacional de Desenvolvimento Científico e Tecnológico and Fundação de Amparo à Pesquisa do Estado do Rio de Janeiro. The authors also thank the Núcleo de Microscopia e Microanálise da Coordenação de Programas de Pós-Graduação em Engenharias/ Universidade Federal do Rio de Janeiro (COPPE/UFRJ) for the microscopy analysis (TEM and SEM).

REFERENCES

1. Miyasaka, K.; Watanabe, K.; Jojima, E.; Ainda, H.; Sumita, M.; Ishikawa, K. *J. Mater. Sci.* **1982**, *17*, 1610.
2. Gubels, F.; Jerome, R.; Teyssie, P.; Vanlathem, E.; Deltour, R.; Calderone, A. *Macromolecules* **1994**, *27*, 1972.
3. Sumita, M.; Sakata, K.; Asai, S.; Miyasaka, K.; Nakagawa, H. *Polym. Bull.* **1991**, *25*, 265.
4. Asai, S.; Sakata, K.; Sumita, M.; Miyasaka, K. *Polym. J.* **1992**, *24*, 415.
5. Pisitsak, P.; Magaraphan, R.; Jana, S. C. *J. Nanomater.* **2012**, 642080.
6. Fenouillot, F.; Cassagnau, P.; Majesté, J. C. *Polymer* **2009**, *50*, 1333.
7. Plattier, J.; Benyahia, L.; Dorget, M.; Niepceron, F.; Tassin, J. F. *Polymer* **2015**, *59*, 260.
8. Zhang, C.; Yi, X. S.; Yui, H.; Asai, S.; Sumita, M. *Mater. Lett.* **1998**, *36*, 186.
9. Wen, S. H.; Chung, D. D. L. *Carbon* **2007**, *45*, 263.
10. Zhang, C.; Han, H. F.; Yi, X. S.; Asai, S.; Sumita, M. *Compos. Interfaces* **1999**, *6*, 227.
11. Huang, C. Y.; Wu, C. C. *Eur. Polym. J.* **2000**, *36*, 2729.
12. Madani, M. *J. Polym. Res.* **2010**, *17*, 53.
13. Rahaman, M.; Chaki, T. K.; Khastgir, D. *J. Mater. Sci.* **2011**, *46*, 3989.
14. Rahaman, M.; Chaki, T. K.; Khasgir, D. *Polym. Compos.* **2011**, *32*, 1790.
15. Rohini, R.; Bose, S. *ACS Appl. Mater. Interfaces* **2014**, *6*, 11302.
16. Han, I. S.; Lee, Y. K.; Lee, H. S.; Yoon, H. G.; Kim, W. N. *J. Mater. Sci.* **2014**, *49*, 4522.
17. Pawar, S. P.; Pattabhi, K.; Bose, S. *RSC Adv.* **2014**, *4*, 18842.
18. Al-Saleh, M. H.; Sundararaj, U. *Macromol. Mater. Eng.* **2008**, *293*, 621.
19. Moreira, A. C. F.; Cario, F. O., Jr.; Soares, B. G. *J. Appl. Polym. Sci.* **2003**, *89*, 386.
20. Wu, S. Polymer Interface and Adhesion; Marcel Dekker: New York, **1982**.
21. Surface tension values of some common test liquids for surface energy analysis. http://www.surface-tension.de. Accessed on 24 June 2015.
22. Min, C.; Yu, D.; Cao, J.; Wang, G.; Feng, L. *Carbon* **2013**, *55*, 116.
23. Yang, Q. Q.; Liang, J. Z. *J. Appl. Polym. Sci.* **2010**, *117*, 1998.
24. Aral, B. K.; Kalyon, D. M. *J. Rheol.* **1997**, *41*, 599.
25. Le Meins, J. F.; Moldenaers, P.; Mewis, J. *Ind. Eng. Chem. Res.* **2002**, *41*, 6297.
26. Mao, C.; Zhu, Y.; Jiang, W. *ACS Appl. Mater. Interfaces* **2012**, *4*, 5281.

27. Hwang, T. Y.; Yoo, Y.; Lee, J. W. *Rheol. Acta* **2012**, *51*, 623.
28. Li, R. M.; Yu, W.; Zhou, C. X. *Polym. Bull.* **2006**, *56*, 455.
29. Joo, J.; Lee, C. Y. *J. Appl. Phys.* **2000**, *88*, 513.
30. Schulz, R. B.; Plantz, V. C.; Brush, D. R. *IEEE Trans.* **1988**, *30*, 187.
31. Al-Saleh, M. H.; Sundararaj, U. *Carbon* **2009**, *47*, 1738.
32. Chung, D. D. L. *J. Mater. Eng. Perform.* **2000**, *9*, 350.
33. Das, N. C.; Khastgir, D.; Chaki, T. K.; Chakraborty, A. *J. Elast. Plast.* **2002**, *34*, 199.
34. Liu, Z.; Bai, G.; Huang, Y.; Ma, Y.; Du, F.; Li, F.; Guo, T.; Chen, Y. *Carbon* **2007**, *45*, 821.